EDGE ARTICLE

Check for updates

All publication charges for this article have been paid for by the Royal Society of Chemistry

Dynamic bond interactions fine-tune the properties of multiple resonance emitters towards highly efficient narrowband green OLEDs†

Yang Zou, [ID] Mingxin Yu, Jingsheng Miao,* Taian Huang, Shuokun Liao, Xiaosong Cao [ID] and Chuluo Yang [ID]

Multiple resonance (MR) molecules based on a B/N polycyclic aromatic framework are the cutting-edge materials in the field of organic light-emitting diodes (OLEDs) owing to their superb photophysical properties. Tailoring the MR molecular framework with various functional groups toward ideal properties has become an emerging topic in the field of materials chemistry. Dynamic bond interactions are versatile and powerful tools in regulating the properties of materials. Herein, the pyridine moiety, which presents high affinity to form dynamic bond interactions such as hydrogen bonds and N→B dative bonds, was introduced into the MR framework for the first time, and the designed emitters are synthesized in a feasible way. The introduction of the pyridine moiety not only maintained the conventional MR properties of the emitters, but also endowed the emitters with tunable emission spectra, narrowed emission, enhanced photoluminescence quantum yield (PLQY), and intriguing supramolecular assembly in the solid state. Thanks to the overall superior properties brought by the hydrogen-bond promoted molecular rigidity, green OLEDs based on the emitter exhibit excellent device performance with external quantum efficiency (EQE) up to 38% and a small FWHM of 26 nm, together with good roll-off performance.

Introduction

Multiple resonance (MR) molecules based on a boron–nitrogen (BN) polycyclic framework are the most alluring emitters for organic light-emitting diodes (OLEDs). The rigid molecular architecture as well as the unique frontier molecular orbitals (FMOs) localized by boron and nitrogen atoms enable point to point transitions, which lead to high photoluminescence quantum yield (PLQY), small singlet-triplet splitting energy (ΔE_{ST}), and most importantly, distinctive narrowband emission with a small full width at half maximum (FWHM). Since the pioneering work by Hatakeyama *et al.*,[1] a number of high-performance MR emitters with cutting-edge device performances have been reported.[2]

Compared to the large number of well-established donor–acceptor type thermally activated delayed fluorescence (TADF) emitters, the newly developed MR emitters demonstrated a much more structural derivatization limit. And tailoring MR

emitters toward ideal properties such as high color-purity,[3] regulated molecular packing[4] and accelerated intersystem crossing rate,[5] has been a long-standing goal ever since their discovery. High color-purity is associated with a suitable emission wavelength and narrow FWHM. Generally, the emission wavelength of the emitters could be tuned by manipulating the intramolecular charge transfer (ICT) state[3] and the degree of conjugation of the molecule, and the FWHM can be narrowed by rigidifying the molecular skeleton.[6] So far, based on this molecular design principle, and by integrating MR molecules with varies donors,[7] acceptors[8] or conventional polycyclic hydrocarbon building blocks,[9] MR emitters displaying blue, green, yellow, red[10] and even near infrared[11] emission have been reported.

From the monomolecular point of view, a planar and rigid molecular framework is essential for BN-based MR emitters in realizing high PLQY and narrowband emission, because it can minimize the molecular structural deformation in the excited state. On the other hand, from the supramolecular perspective, most BN-based MR molecules that possess a planar and rigid molecular framework exhibit a strong π–π stacking tendency to form non-emissive aggregates at high concentrations owing to their rigid and planar structure.[3,8,12] Therefore, during device fabrication, a low doping concentration (1%) was essential to ensure good device performance. Until now, only a handful of MR emitters free from π–π stacking have been reported by
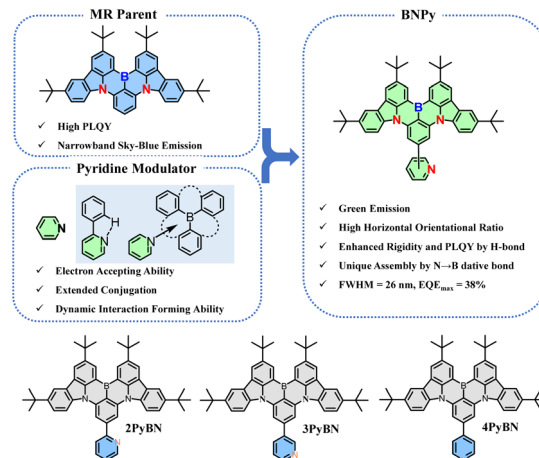
constructing a sterically hindered molecular structure.[4] And thus, apart from the emission color tuning, exploring MR molecules with unique self-assembly could be intriguing from both material and supramolecular perspectives.

Dynamic bond interactions, such as π–π stacking, hydrogen bonding (H-bonding),[13] N→B dative bonding, *etc.*, have played an important role in regulating the material properties. For example, inter- and intramolecular H-bonding can be used to lock the molecular conformation, thereby enhancing the PLQY of the material by minimizing the non-radiative decay.[14] And N→B dative bonding can be used to construct rigid mono-molecular and supramolecular structures with intriguing assembly and material processability.[15] Compared to the bottom-up strategies associated with precise synthesis and possible solubility issues, the reversible dynamic bond inter-actions offer a more versatile strategy to manipulate the monomolecular conformation of the material as well as its supramolecular aggregation behavior.

Pyridine derivatives, which represent one of the most extensively investigated building blocks with electron accepting nature, are particularly appealing to construct host,[16] charge transporting[17] and light-emitting materials[18] for OLEDs. In addition, with the lone pair located on the nitrogen atom, pyridine derivatives are well-known moieties that are widely used in the fields of materials chemistry, and supramolecular and coordination chemistry[19] owing to their ability to form H-bonding, N→B dative bonding, or metal-containing complexes. In this context, we envisioned that the integration of the pyridine building block into the conventional MR framework could fine-tune the optical properties as well as the packing behavior of the emitter, benefiting from the electron withdrawing nature and non-covalent bond forming ability of the pyridine moiety. In this contribution, the pyridine moiety was introduced into a typical BN-based MR molecular frame-work for the first time. The introduction of the pyridine moiety not only allows for fine-tuning of the emission wavelength, the FWHM, and the PLQY of the emitter, but also greatly changes the supramolecular packing behavior, depending on the substitution pattern. Eventually, green OLEDs with high external quantum efficiency (EQE) up to 38% and a FWHM as narrow as 26 nm were realized by incorporating these molecules as emitters into devices. The role of pyridine rings, and the impact of the substitution pattern on the structure–property correlations of the materials were elucidated.

Results and discussion

The molecular design and the chemical structures of the emitters are depicted in Scheme 1, and the synthetic route is provided in Scheme S1 (see ESI†). All three emitters possess the same well-known BNCz parent moiety, while the pyridine ring was grafted onto the *para*-position of the boron atom in the *ortho*-, *meta*-, or *para*-substitution pattern, resulting in three emitters namely 2PyBN, 3PyBN and 4PyBN, respectively. Initially, the emitters were synthesized based on the well-established approach (route A, Scheme S1†), in which pyridine was connected to the substrate and then subjected to lithium mediated borylation. However, the

Scheme 1 The molecular design and the chemical structures of 2PyBN, 2PyBN and 2PyBN.

reaction resulted in an unisolable mixture. The complexation of the borylation was probably due to the coordination of the pyri-dine ring with boron tribromide. Therefore, the optimized route (route B, Scheme S1†) was proposed based on the post-functionalization approach. In this route, the dibromo compound **1** was selectively borylated to give the key intermediate BNCz-Br, and then subjected to CuCl assisted Suzuki–Miyaura coupling[20] to give the desired product. The optimized route resulted in the clean product with high yield, and it required a much less tedious purification technique. This post-functionalization approach also allowed for mass production of the MR emitters with varying functionalities with good functional group tolerance. Chemical structures of the intermediates and final products were fully identified by nuclear magnetic reso-nance (NMR) spectroscopy (Fig. S1–S8, see ESI†) and electron spray ionization mass spectrometry (HR-ESI-MS). The high decomposition temperatures (T_ds) of over 400 °C acquired from thermogravimetric analysis (TGA, Fig. S9†) indicated good stability of the emitter, allowing them to be processed by the vacuum deposition technique for device fabrication.

Single crystals of 2PyBN and 4PyBN were cultivated by evapo-rating ethanol into their dichloromethane solution. As shown in Fig. 1, despite the similar BNCz motif, the two molecules revealed quite different monomolecular conformations and distinct supramolecular packing patterns. 2PyBN displayed a more planar conformation than 4PyBN. The small dihedral angle of 19° between the BNCz core and the pyridyl substitute, and the short distance of 2.47 Å between the nitrogen and the adjacent hydrogen atom indicated intramolecular H-bonds in the 2PyBN molecule. Such H-bond promoted planar molecular conformation was beneficial for realizing a high PLQY and small FWHM due to the enhancement of molecular rigidity and minimization of deformation in the excited state for the emitter. Surprisingly, the tiny difference in the substitution pattern for 2PyBN and 4PyBN showed profound impact on their packing behavior. Like most of the BN-based MR emitters, 2PyBN revealed conventional π–π stacking with a close distance shorter than 3.3 Å. In sharp
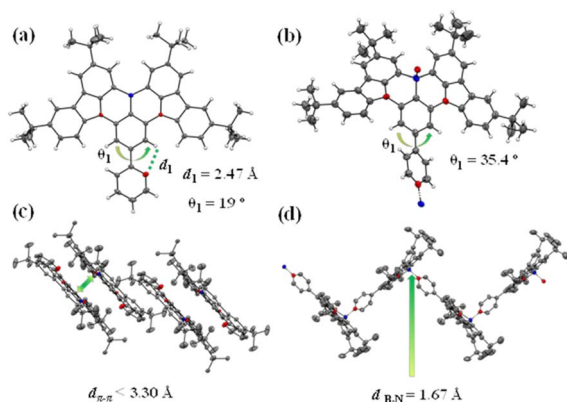
Fig. 1 Single-crystal X-ray structures of (a) 2PyBN (CCDC 2194020) and (b) 4PyBN (CCDC 2194021) with thermal ellipsoids at the 50% probability level. Solid-state packing of 2PyBN (c) and 4PyBN (d) in the solid state (hydrogen atoms were omitted for clarity).

contrast, the pyridine substituents in 4PyBN interacted with the boron atom in the neighboring molecule by forming a N→B dative bond, resulting in a novel zig–zag shaped head-to-tail coordination polymer. It should be noted that such a coordination polymer existing in the solid state would dissociate in solution, as proved by the almost unchanged concentration dependent UV-vis and slightly red-shifted narrowband fluorescence spectra in toluene solution (Fig. S11†). Although such pyridine–triarylboron interactions had been reported and been used for material design and processing, they were only realized by adding pyridine externally to a triaryl boron compound.[15a,15c] Thus, this is among the very few examples[19d] such unique assembly had been realized by combining triaryl boron and pyridine motifs in a single molecule.

The optimal structures acquired from computational simulation were in good agreement with their crystal structures as well, according to the density functional theory (DFT) calculations using time dependent density function theory (TD-DFT). As shown in Fig. 2, the BNCz moiety in the three emitters all adopted a semi-planar structure, and the pyridine ring was twisted to the BNCz moiety for 3PyBN and 4PyBN, while 2PyBN revealed a more
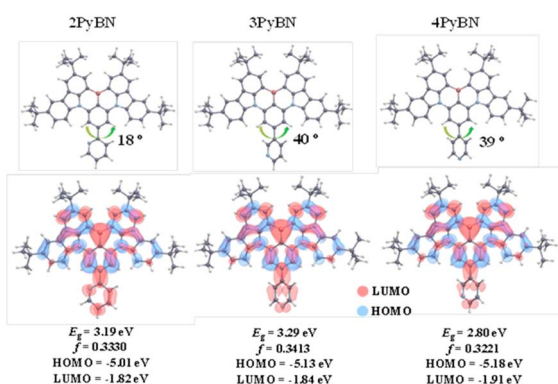
planar structure. In addition, all three emitters demonstrated typical MR-type FMO distributions with high oscillation strength, and the lowest unoccupied molecular orbitals (LUMOs) were extended to the pyridine moiety. Because of the increased electron inductive effect for *ortho-* than *para-* and *meta-*substitution patterns, the energy gap (E_g) was gradually lowered from 3PyBN to 4PyBN, and then 2PyBN, indicating tunable emission.

Despite of the different substitution pattern of pyridine moiety, all three emitters showed typical MR-type photophysical behavior. As shown in Fig. 3 and summarized in Table 1, in toluene solution, all three emitters displayed a local π–π* and n–π* transition absorption band at 280–350 nm, along with an ICT band from 450–500 nm. Because the electron withdrawing ability of pyridine varies with the substitution pattern,[8] the absorption maxima (λ_{abs}) of ICT bands and the emission maxima were gradually red-shifted in the order of 3PyBN, 4PyBN and 2PyBN, which were highly coincidental with the theoretical prediction. Notably, benefiting from the enhanced molecular rigidity promoted by intramolecular H-bonds, among the three emitters, 2PyBN showed the smallest FWHM (21 nm, 0.1 eV) in solution, as well as the highest PLQY of 95% in the doped film. When doped in the 1,3-dihydro-1,1-dimethyl-3-(3-(4,6-diphenyl-1,3,5-triazin-2-yl)phenyl)indeno-[2,1-*b*]carbazole (DMIC-TRZ) host, the emitters showed similar emission spectra compared to their toluene solution, except for a slight red-shift and spectral broadening due to the interaction with the host. And small ΔE_{ST}s of ~0.02 eV were determined based on their fluorescence and phosphorescent spectra. The TADF nature of the

Fig. 2 Optimal molecular structures, FMO distributions, and related energies of the emitters.
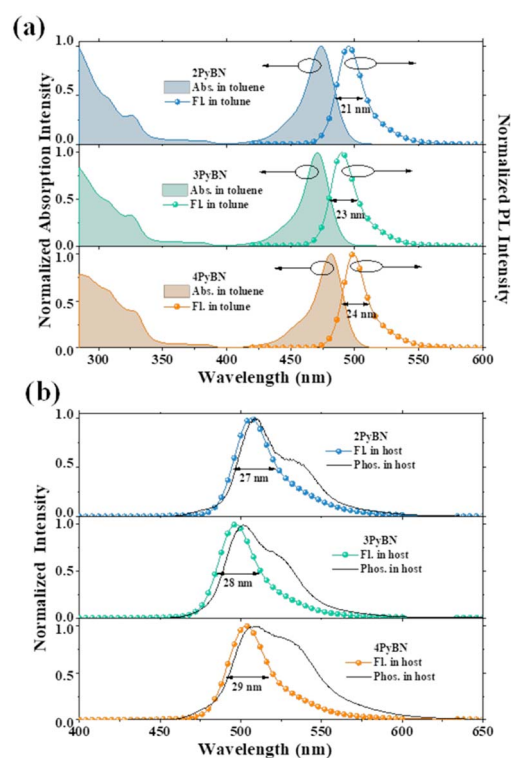

Fig. 3 (a) UV-vis spectra of the emitters in toluene (10^{-5} M), (b) fluorescence and phosphorescence spectra of 1% emitters in DMIC-TRZ.

Table 1 Thermal and physical data of the emitters

Emitter	T_d (°C)	$\lambda_{abs}{}^a$ (nm)	$\lambda_{em}{}^{a,b}$ (nm)	FWHM^a (nm eV^{-1})	PLQY^b (%)	HOMO^c (eV)	LUMO^c (eV)	$S_1{}^d$ (eV)	$T_1{}^d$ (eV)	ΔE_{ST} (eV)	$\Theta_{//}$ (%)
2PyBN	432	481	499/507	21/0.10	94	−5.36	−2.94	2.57	2.55	0.02	95
3PyBN	429	471	490/497	23/0.11	90	−5.42	−2.95	2.62	2.59	0.03	96
4PyBN	424	474	495/506	24/0.12	86	−5.43	−2.99	2.60	2.58	0.02	96

^{a} Measured in toluene solutions (10^{-5} M) at 298 K. ^{b} Measured for 1% emitter doped in the DMIC-TRZ host. ^{c} HOMOs were calculated from CV (see Fig. S10); LUMO = HOMO + E_g^{opt}. ^{d} Calculated from the onset of the fluorescence spectra and phosphorescence at 77 K.

emitters was further confirmed by the bi-exponential decay in transient photoluminescence decay spectra (Fig. S12†), in which the prompt and delayed component lifetimes were 9.4 ns/15.9 μs, 8.5 ns/13.6 μs and 8.2 ns/12.4 μs for 2PyBN, 3PyBN and 4PyBN, respectively. Based on the calculation from photophysical data (Table S1†), all three emitters exhibited a very fast radiative decay rate (k_r) of over 1×10^8 s^{-1}, while 2PyBN showed the smallest non-radiative rate (k_{nr}) among the three emitters owing to its most rigid molecular structure. Moreover, a high horizontal molecular orientation ratio ($\Theta_{//}$) was essential for boosting the EQEs of the EL devices by increasing the optical out-coupling factor; the pyridine substituent also boosted the horizontal molecular orientation ratios ($\Theta_{//}$s) by enlarging the plane of the molecular framework, and all three emitters showed a high $\Theta_{//}$ of 96%, which was much higher than that of the parent BNCz molecule (74%),[3] as proved by angle-dependent p-polarized photoluminescence (PL) spectra (Fig. S13†).

The excellent optical properties of the molecules including high PLQYs, small ΔE_{ST} and high $\Theta_{//}$s indicated that they were ideal emitters for OLEDs. To explore their electroluminescence (EL) performances, EL devices were fabricated with the following device configuration: ITO/HAT-CN (5 nm)/TAPC (30 nm)/TCTA (15 nm)/mCBP (10 nm)/EML/POT2T (20 nm)/ANT-BIZ (30 nm)/Liq (2 nm)/Al (100 nm). In the device configuration, dipyrazino[2,3-f:2′,3′-h]quinoxaline-2,3,6,7,10,11-hexacarbonitrile (HATCN) served as a hole injection layer; 1,1-bis((di-4-tolylamino)phenyl)-cyclohexane (TAPC) and (1-(4-(10-([1,1′-biphenyl]-4-yl)anthracen-9-yl)phenyl)-2-ethyl-1H-benzo[d]-imidazole) (ANT-BIZ) were applied as hole- and electron-transport layers, respectively; 1,3-di(9H-carbazol-9-yl)benzene (mCBP) and 2,4,6-tris[3-(diphenylphosphinyl)phenyl]-1,3,5-triazine (POT2T) served as exciton-blocking layers; DMIC-TRZ was used as the host due to its balanced charge transporting properties.[21] The emitter was doped into the host at the

optimized doping concentrations of 1% or 5% to serve as the emitting layer (EML). The detailed device structure and chemical structures of the materials are shown in Fig. S14.†

As shown in Fig. S14† and summarized in Table 2, all devices displayed characteristic narrowband EL spectra identical to the emitters' PL spectra, indicating complete energy transfer from the host to the emitters. The 2PyBN-based green OLEDs exhibited the highest EQE$_{max}$ of 37.1%, the narrowest emission, and the highest brightness of 75 000 cd m^{-2}, together with the highest power and current efficiency among the three devices. Further increasing the doping concentration of the emitter to 5% led to decreased device efficiency and spectral broadening (Fig. S15 and Table S3†) due to unwanted aggregation caused quenching. The good device performance correlated with the superior photophysical properties of 2PyBN among the three emitters, which unambiguously proved the advantages of the intramolecular H-bond promoted rigidity in the material design.

To further suppress the efficiency roll-off caused by the relative slow reverse intersystem crossing rate of the emitters, sensitized devices were also fabricated, in which 2,3,4,5,6-pentakis(3,6-di-$tert$-butyl-9H-carbazol-9-yl)benzonitrile (5TCzBN) was introduced into the EML with a doping concentration of 20% to serve as the sensitizer.[8] As shown in Fig. 4 and summarized in Table 2, with the help of the sensitizer, all three devices demonstrated improved performances with boosted efficiencies of EQE over 36% and higher brightness. The 2PyBN-based device, in particular, exhibited the best performances with a L_{max} of 89 800 cd m^{-2} and the smallest FWHM of 26 nm, and its EQE$_{max}$ of 38% was also among the highest values for green OLEDs with a similar device configuration (see Table S4† for comparison).[4,9b,22] The high EQEs were highly coincidental with theoretical efficiencies as predicted by optical simulation. In addition, the sensitized

Table 2 Summary of the EL device data

EML	$V_{on}{}^a$ (V)	L_{max} (cd m^{-2})	λ_{EL} (nm)	FWHM (nm)	EQE^b (%)	PE$_{max}$ (lm W^{-1})	CE$_{max}$ (cd A^{-1})	CIE (x, y)
2PyBN	2.4	75 000	505	26	37.1/18.0/7.7	139.6	106.7	0.12, 0.65
3PyBN	2.4	51 000	494	27	33.0/15.3/6.5	90.3	69.0	0.10, 0.48
4PyBN	2.4	61 000	501	27	35.5/16.6/6.5	113.9	87.0	0.11, 0.57
2PyBN^c	2.4	89 800	501	26	38.0/29.4/17.2	108.8	96.9	0.12, 0.57
3PyBN^c	2.4	79 000	492	28	37.8/30.0/16.9	87.6	77.1	0.11, 0.45
4PyBN^c	2.4	83 900	498	29	36.8/27.5/15.8	98.6	86.5	0.11, 0.53

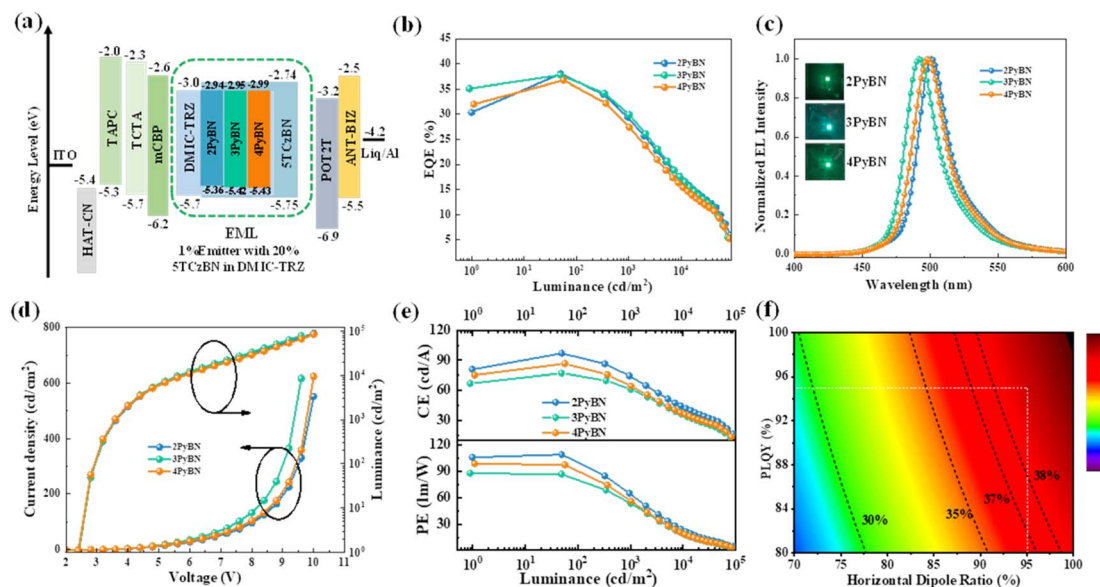^{a} Turn-on voltage. ^{b} Maximum, at 1000 and 10 000 cd m^{-2}. ^{c} With 20% 5TCzBN as the sensitizer.

Fig. 4 (a) Device configuration and the energy level diagrams, (b) EQE *versus* luminance curves, (c) the EL spectra recorded at 1000 cd m^{-2} and the images of the devices, (d) luminescence and current density *versus* voltage characteristics, (e) CE/PE *versus* luminance curves, and (f) theoretical device efficiency with respect to PLQY and horizontal orientation factor *via* optical simulation.

device also showed low efficiency roll-off with the EQE maintained at ~30% and 17% at a high brightness of 1000 cd m^{-2} and 10 000 cd m^{-2}, respectively.

Conclusions

In summary, three novel isomeric MR emitters were designed and synthesized by integrating the pyridine moiety with a conventional BN-based MR framework. The introduction of the pyridine moiety not only enabled fine-tuning of the emission wavelength of the emitters based on the substitution pattern, but also brought about a series of intriguing properties such as narrowed emission, elevated PLQY, and unique supramolecular assembly, realized by dynamic bond interactions including H-bonds and N→B dative bonds. With the help of the intrinsic fast k_r, the high $\Theta_{//}$, and the high PLQY brought by H-bond promoted molecular rigidity, narrowband green OLEDs with a FWHM of 26 nm and a high EQE of 38% were achieved. The facile synthesis, the dynamic bond fine-tuned structure–property relationship, and the excellent devices in this work would provide a new approach for future structure derivatization of MR molecules in the fields of both supramolecular and materials chemistry.

Data availability

All data supporting this study are available from article and ESI.†

Author contributions

M. Yu, T. Huang and S. Liao synthesized the materials. M. Yu and X. Cao analyzed the data. Y. Zou validated the data and wrote the manuscript. J. Miao fabricated the device and

supervised the project. C. Yang conceived the original idea. All authors contributed to the discussion of the results.

Conflicts of interest

There are no conflicts to declare.

Acknowledgements

Notes and references

1 (*a*) T. Hatakeyama, K. Shiren, K. Nakajima, S. Nomura, S. Nakatsuka, K. Kinoshita, J. Ni, Y. Ono and T. Ikuta, *Adv. Mater.*, 2016, **28**, 2777; (*b*) K. Matsui, S. Oda, K. Yoshiura, K. Nakajima, N. Yasuda and T. Hatakeyama, *J. Am. Chem. Soc.*, 2018, **140**, 1195; (*c*) Y. Kondo, K. Yoshiura, S. Kitera, H. Nishi, S. Oda, H. Gotoh, Y. Sasada, M. Yanai and T. Hatakeyama, *Nat. Photonics*, 2019, **13**, 678; (*d*) N. Ikeda, S. Oda, R. Matsumoto, M. Yoshioka, D. Fukushima, K. Yoshiura, N. Yasuda and T. Hatakeyama, *Adv. Mater.*, 2020, **32**, 2004072.

2 (*a*) H. Lee, D. Karthik, R. Lampande, J. H. Ryu and J. H. Kwon, *Front. Chem.*, 2020, **8**, 373; (*b*) S. Madayanad Suresh, D. Hall, D. Beljonne, Y. Olivier and E. Zysman-Colman, *Adv. Funct. Mater.*, 2020, **30**, 1908677;

(c) J. M. Teng, Y. F. Wang and C. F. Chen, *J. Mater. Chem. C*, 2020, **8**, 11340.

3 M. Yang, I. S. Park and T. Yasuda, *J. Am. Chem. Soc.*, 2020, **142**, 19468.

4 (a) Y. Zhang, J. Wei, D. Zhang, C. Yin, G. Li, Z. Liu, X. Jia, J. Qiao and L. Duan, *Angew. Chem., Int. Ed.*, 2022, **61**, e202113206; (b) P. Jiang, J. Miao, X. Cao, H. Xia, K. Pan, T. Hua, X. Lv, Z. Huang, Y. Zou and C. Yang, *Adv. Mater.*, 2022, **34**, e2106954; (c) Y. K. Qu, D. Y. Zhou, F. C. Kong, Q. Zheng, X. Tang, Y. H. Zhu, C. C. Huang, Z. Q. Feng, J. Fan, C. Adachi, L. S. Liao and Z. Q. Jiang, *Angew. Chem., Int. Ed.*, 2022, **61**, e202201886.

5 (a) M. Nagata, H. Min, E. Watanabe, H. Fukumoto, Y. Mizuhata, N. Tokitoh, T. Agou and T. Yasuda, *Angew. Chem., Int. Ed.*, 2021, **60**, 20280; (b) I. S. Park, H. Min and T. Yasuda, *Angew. Chem., Int. Ed.*, 2022, **61**, e202205684.

6 J. Liu, Y. Zhu, T. Tsuboi, C. Deng, W. Lou, D. Wang, T. Liu and Q. Zhang, *Nat. Commun.*, 2022, **13**, 4876.

7 (a) M. Yang, S. Shikita, H. Min, I. S. Park, H. Shibata, N. Amanokura and T. Yasuda, *Angew. Chem., Int. Ed.*, 2021, **60**, 23142; (b) Y. Qi, W. Ning, Y. Zou, X. Cao, S. Gong and C. Yang, *Adv. Funct. Mater.*, 2021, **31**, 2102017; (c) Y. Xu, C. Li, Z. Li, Q. Wang, X. Cai, J. Wei and Y. Wang, *Angew. Chem., Int. Ed.*, 2020, **59**, 17442.

8 Y. Zhang, D. Zhang, J. Wei, Z. Liu, Y. Lu and L. Duan, *Angew. Chem., Int. Ed.*, 2019, **58**, 16912.

9 (a) Y. Zhang, D. Zhang, J. Wei, X. Hong, Y. Lu, D. Hu, G. Li, Z. Liu, Y. Chen and L. Duan, *Angew. Chem., Int. Ed.*, 2020, **59**, 17499; (b) Y. Xu, Q. Wang, J. Wei, X. Peng, J. Xue, Z. Wang, S. J. Su and Y. Wang, *Angew. Chem., Int. Ed.*, 2022, **61**, e202204652; (c) Y. Zhang, G. Li, L. Wang, T. Huang, J. Wei, G. Meng, X. Wang, X. Zeng, D. Zhang and L. Duan, *Angew. Chem., Int. Ed.*, 2022, **61**, e202204652.

10 (a) Y. Zou, J. Hu, M. Yu, J. Miao, Z. Xie, Y. Qiu, X. Cao and C. Yang, *Adv. Mater.*, 2022, **34**, e2201442; (b) X. Cai, Y. Xu, Y. Pan, L. Li, Y. Pu, X. Zhuang, C. Li and Y. Wang, *Angew. Chem., Int. Ed.*, 2022, e202216473.

11 (a) J. K. Li, X. Y. Chen, Y. L. Guo, X. C. Wang, A. C. Sue, X. Y. Cao and X. Y. Wang, *J. Am. Chem. Soc.*, 2021, **143**, 17958; (b) Y. Zhang, D. Zhang, T. Huang, A. J. Gillett, Y. Liu, D. Hu, L. Cui, Z. Bin, G. Li, J. Wei and L. Duan, *Angew. Chem., Int. Ed.*, 2021, **60**, 20498.

12 Y. C. Xu, Z. Cheng, Z. Q. Li, B. Y. Liang, J. X. Wang, J. B. Wei, Z. L. Zhang and Y. Wang, *Adv. Opt. Mater.*, 2020, **8**, 1902142.

13 (a) Y. Zou, X. Ji, J. Cai, T. Yuan, D. J. Stanton, Y.-H. Lin, M. Naraghi and L. Fang, *Chem*, 2017, **2**, 139–152; (b) D. González-Rodríguez and A. P. H. J. Schenning, *Chem. Mater.*, 2011, **23**, 310–325; (c) Y. Shi, K. Wang, Y. Tsuchiya, W. Liu, T. Komino, X. Fan, D. Sun, G. Dai, J. Chen, M. Zhang, C. Zheng, S. Xiong, X. Ou, J. Yu, J. Jie, C.-S. Lee,

C. Adachi and X. Zhang, *Mater. Horiz.*, 2020, **7**, 2734; (d) P. Rajamalli, N. Senthilkumar, P. Y. Huang, C. C. Ren-Wu, H. W. Lin and C. H. Cheng, *J. Am. Chem. Soc.*, 2017, **139**, 10948.

14 (a) Y. Xu, C. Li, Z. Li, J. Wang, J. Xue, Q. Wang, X. Cai and Y. Wang, *CCS Chem.*, 2021, 2077; (b) W. Yuan, H. Yang, C. Duan, X. Cao, J. Zhang, H. Xu, N. Sun, Y. Tao and W. Huang, *Chem*, 2020, **6**, 1998.

15 (a) S. Saito, K. Matsuo and S. Yamaguchi, *J. Am. Chem. Soc.*, 2012, **134**, 9130; (b) X. Shao, M. Liu, J. Liu and L. Wang, *Angew. Chem., Int. Ed.*, 2022, **61**, e202205893; (c) K. Matsuo, S. Saito and S. Yamaguchi, *Angew. Chem., Int. Ed.*, 2016, **55**, 11984; (d) C. Zhu, X. Ji, D. You, T. L. Chen, A. U. Mu, K. P. Barker, L. M. Klivansky, Y. Liu and L. Fang, *J. Am. Chem. Soc.*, 2018, **140**, 18173; (e) H. Zhang, Y. Li, L. Chen, Y. Yang, H. Lin, S. Xiang, B. Chen and Z. Zhang, *Chem*, 2023, **9**, 242; (f) W. Wang, L. Wang, F. Du, G.-D. Wang, L. Hou, Z. Zhu, B. Liu and Y.-Y. Wang, *Chem. Sci.*, 2023, **14**, 533.

16 (a) S.-J. Su, H. Sasabe, T. Takeda and J. Kido, *Chem. Mater.*, 2008, **20**, 1691; (b) F. Wang, L. Zhang, W. Han, Z. Bin and J. You, *Angew. Chem., Int. Ed.*, 2022, **61**, e202205380.

17 (a) S.-J. Su, Y. Takahashi, T. Chiba, T. Takeda and J. Kido, *Adv. Funct. Mater.*, 2009, **19**, 1260; (b) H. Ye, D. Chen, M. Liu, S.-J. Su, Y.-F. Wang, C.-C. Lo, A. Lien and J. Kido, *Adv. Funct. Mater.*, 2014, **24**, 3268.

18 (a) Y. K. Chen, J. Jayakumar, C. M. Hsieh, T. L. Wu, C. C. Liao, J. Pandidurai, C. L. Ko, W. Y. Hung and C. H. Cheng, *Adv. Mater.*, 2021, **33**, e2008032; (b) J. Li, W.-C. Chen, H. Liu, Z. Chen, D. Chai, C.-S. Lee and C. Yang, *J. Mater. Chem. C*, 2020, **8**, 602.

19 (a) A. Wu, Y. Guo, X. Li, H. Xue, J. Fei and J. Li, *Angew. Chem., Int. Ed.*, 2021, **60**, 2099; (b) Q. Zheng, S. L. Rood, D. K. Unruh and K. M. Hutchins, *CrystEngComm*, 2018, **20**, 6377; (c) J. Trouve, P. Zardi, S. Al-Shehimy, T. Roisnel and R. Gramage-Doria, *Angew. Chem., Int. Ed.*, 2021, **60**, 18006; (d) J. He, F. Rauch, A. Friedrich, J. Krebs, I. Krummenacher, R. Bertermann, J. Nitsch, H. Braunschweig, M. Finze and T. B. Marder, *Angew. Chem., Int. Ed.*, 2021, **60**, 4833.

20 J. Z. Deng, D. V. Paone, A. T. Ginnetti, H. Kurihara, S. D. Dreher, S. A. Weissman, S. R. Stauffer and C. S. Burgey, *Org. Lett.*, 2009, **11**, 345.

21 D. Zhang, C. Zhao, Y. Zhang, X. Song, P. Wei, M. Cai and L. Duan, *ACS Appl. Mater. Interfaces*, 2017, **9**, 4769.

22 (a) F. Liu, Z. Cheng, Y. Jiang, L. Gao, H. Liu, H. Liu, Z. Feng, P. Lu and W. Yang, *Angew. Chem., Int. Ed.*, 2022, **61**, e202116927; (b) S. Oda, T. Sugitani, H. Tanaka, K. Tabata, R. Kawasumi and T. Hatakeyama, *Adv. Mater.*, 2022, **34**, e2201778.